

Ultrasensitive and Wide-Bandwidth Thermal Measurements of Graphene at Low Temperatures

Kin Chung Fong* and K. C. Schwab

Applied Physics, California Institute of Technology, MC 128-95, Pasadena, California 91125, USA

(Received 9 April 2012; published 30 July 2012; corrected 3 August 2012)

At low temperatures, the electron gas of graphene is expected to show both very weak coupling to thermal baths and rapid thermalization, properties which are desirable for use as a sensitive bolometer. We demonstrate an ultrasensitive, wide-bandwidth measurement scheme based on Johnson noise to probe the thermal-transport and thermodynamic properties of the electron gas of graphene, with a resolution of $2 \text{ mK}/\sqrt{\text{Hz}}$ and a bandwidth of 80 MHz. We have measured the electron-phonon coupling directly through energy transport, from 2–30 K and at a charge density of $2 \times 10^{11} \text{ cm}^{-2}$. We demonstrate bolometric mixing and utilize this effect to sense temperature oscillations with a period of 430 ps and determine the heat capacity of the electron gas to be $2 \times 10^{-21} \text{ J}/(\text{K} \cdot \mu\text{m}^2)$ at 5 K, which is consistent with that of a two-dimensional Dirac electron gas. These measurements suggest that graphene-based devices, together with wide-bandwidth noise thermometry, can generate substantial advances in the areas of ultrasensitive bolometry, calorimetry, microwave and terahertz photo-detection, and bolometric mixing for applications in fields such as observational astronomy and quantum information and measurement.

DOI: [10.1103/PhysRevX.2.031006](https://doi.org/10.1103/PhysRevX.2.031006)

Subject Areas: Graphene, Mesoscopics, Photonics

I. INTRODUCTION

Graphene is a material with remarkable electronic properties [1] and exceptional thermal-transport properties near room temperature, which have been well examined and understood [2]. In fact, recent experiments have shown that graphene exhibits one of the highest phononic thermal conductivities of all measured materials [3]. However, at low temperatures, the thermodynamic and thermal-transport properties are much less well explored [4] and somewhat surprisingly, due to the single atomic thickness, low electron density, linear band structure, and weak electron-phonon coupling, the electron gas of graphene is expected to exhibit extreme thermal isolation [5–7].

The very weak thermal coupling combined with exceptionally small electronic heat capacity of graphene leads to projections for very high sensitivity as both a bolometer [8,9] and as a calorimeter [10,11]. As is typical with extremely sensitive sensors, a device readout that has both the sensitivity and sufficiently low measurement backaction to realize the ultimate measurement sensitivity can also be a significant challenge. Because of the thermal sensitivity and the relatively weak dependence of resistance on temperature [12,13], the simplistic use of electrical transport as the readout scheme cannot realize the ultimate sensitivity of graphene, which is given by thermodynamic fluctuations [14,15]. Here, we present a measurement

scheme based upon high-frequency Johnson noise, which provides both wide bandwidth and sensitivity to resolve the fundamental thermal fluctuations, with minimal disturbance to the thermal properties of the sample. This technique should be useful for both thermodynamic studies of graphene [16–19] and for bolometric applications at very low temperatures.

This paper is organized as follows. We present the thermal model of the electron gas of graphene at low temperatures in Sec. II. Section III discusses the Johnson-noise measurement scheme and fundamental limits to the sensitivity. In Sec. IV, we present our measurements, which provide a direct and accurate measurement of the electron-phonon coupling of graphene from 2–30 K, and a measurement of the thermal time constant, and we determine the heat capacity of graphene. Section V explores the expected sensitivity of graphene as a bolometer and as a calorimeter in the temperature range from 10 mK to 10 K. These estimates suggest a number of exciting possibilities: detection of single microwave-frequency photons, photon number resolution, and spectroscopy of terahertz photons [9,20–22].

II. THERMAL MODEL

Figure 1(b) shows the temperature dependence of the expected thermal-conductance channels for the two-dimensional electron gas: coupling to the electrical leads through electron diffusion, G_{WF} , coupling to the lattice, G_{ep} , and coupling to the electromagnetic environment, G_{rad} , where G_{tot} is the sum of all three mechanisms.

Thermal transport through electron diffusion in graphene has not yet been measured and most theories focus on the clean, low-density graphene [16,17]. For doped

*kcfong@caltech.edu

Published by the American Physical Society under the terms of the Creative Commons Attribution 3.0 License. Further distribution of this work must maintain attribution to the author(s) and the published article's title, journal citation, and DOI.

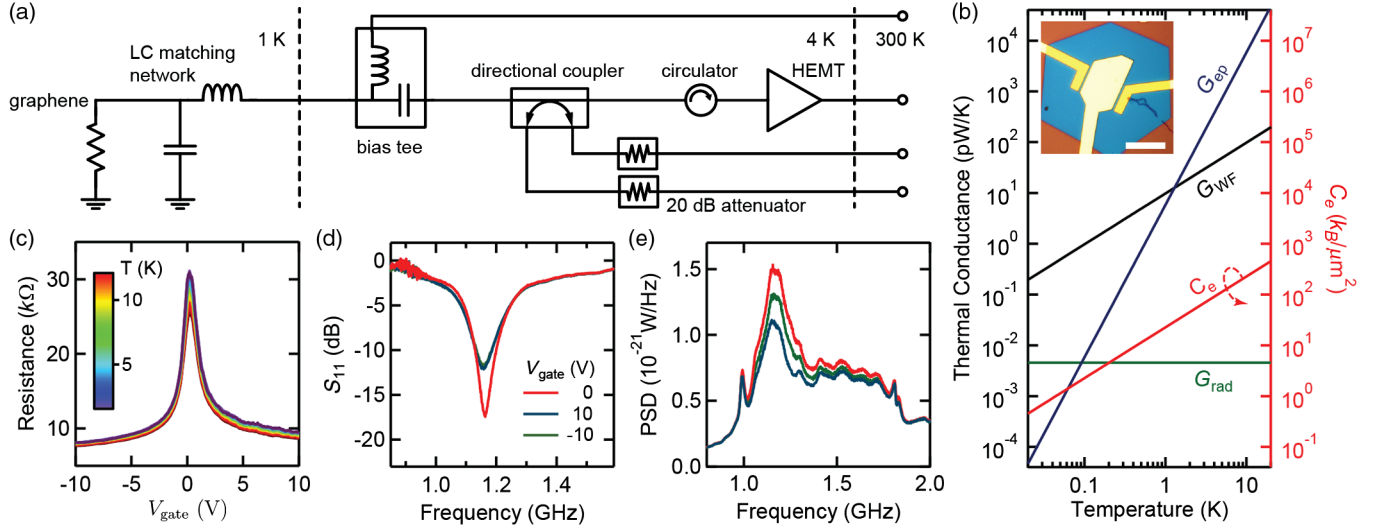


FIG. 1. (a) The measurement circuit: graphene (represented by a resistor), impedance matched with a 1.161 GHz resonant, lithographic LC network (NbTiN film, $T_c = 13.5$ K), and connected to a HEMT amplifier. (b) The expected thermal conductances (G_{WF} , G_{ep} , G_{rad}) and heat capacity versus temperature for a bandwidth of 80 MHz, $n = 10^{11}$ cm $^{-2}$, and $A = 10^{-10}$ m 2 . The inset shows an optical micrograph of the graphene sample. The scale bar is 15 μ m long. (c) The two-terminal resistance of the graphene versus gate voltage, taken from 1.65–12 K. (d) The reflected microwave response versus gate voltage. The absorption dip at 1.161 GHz shows that the graphene is well matched to 50 Ω in an 80-MHz band. (e) Spectra of the measured noise power taken at various sample temperatures, demonstrating the Johnson-noise signal of the graphene in the impedance-matching band.

samples dominated by the disorder potential of the SiO $_2$ substrate [23], such as the sample in this report, we assume the simple Wiedemann-Franz (WF) relationship as a starting point: $G_{WF} = 12L_0T_e/R$, where T_e is the electron temperature, and L_0 and R are the Lorenz constant and the electrical resistance of the sheet, respectively. The prefactor, 12, is the result of the temperature profile developed by uniform ohmic heating and by the presence of the thermal boundary condition of the contacts in a two-terminal device (see comment [14] in Ref. [24] and the Supplemental Material [25]).

The thermal conductance through the emission and absorption of blackbody photons into the electromagnetic environment formed by the electrical measurement system is limited by the quantum of thermal conductance [26], $G_0 = \pi k_B^2 T_e / (6\hbar)$ (where k_B and \hbar are the Boltzmann and Planck constants, respectively), and the bandwidth of the connection to the environment, B : $G_{rad} = G_0(2\pi\hbar B/k_B T_e)$, where B , the bandwidth of the blackbody radiation [27], is assumed to be less than $k_B T_e / (2\pi\hbar)$.

The electron gas can thermalize through the emission and absorption of acoustic phonons [28]. For temperatures below the Bloch-Grüneisen temperature [13,29,30] [$T_{BG} = 2c\pi^{1/2}\hbar v_F n^{1/2} / (v_F k_B) = 33$ K for $n = 10^{11}$ cm $^{-2}$], heat transport between electrons and phonons in a doped sample in the clean limit ($k_p l_e \gg 1$ where k_p and l_e are the phonon wave vector and electron mean-free path, respectively) is expected to follow $\dot{Q} = A\Sigma(T_e^4 - T_p^4)$ [5–7,31], where A is the sample area, $\Sigma = (\pi^{5/2} k_B^4 D^2 n^{1/2}) / (15\rho\hbar^4 v_F^2 c^3)$ is the electron-phonon coupling constant, D is the deformation

potential that characterizes the scattering of electrons by phonons, $v_F = 10^6$ m/s is the Fermi velocity, $c = 20$ km/s is the speed of sound, and n is the charge-carrier density. When $|T_e - T_p| \ll T_p$, the electron-phonon coupling $G_{ep} = 4\Sigma A T^3$. This coupling has been inferred using the temperature dependence of electrical transport for $T > T_{BG}$ at a charge density of $n = 10^{12}$ cm $^{-2}$ [13] and for both $T > T_{BG}$ and $T < T_{BG}$ with a very high charge density, $n \geq 10^{13}$ cm $^{-2}$ [30]. These measurements are consistent with the expected form and magnitude of the coupling.

Through careful engineering of the sample geometry and the coupling to the electrical environment, it is possible to force the graphene to thermalize primarily through the electron-phonon channel, minimizing G_{tot} (see Supplemental Material [25] and Refs. [32–38]) and at very low temperatures, this thermal conductance is expected to be extraordinarily weak [7] (Fig. 1). The thermal modeling of our graphene sample shows that the thermal conductance is expected to be dominated by G_{ep} for temperatures larger than 1 K, and by G_{WF} for $T < 1$ K, as shown in Fig. 1(b). Superconducting leads can be used to block transport through G_{WF} [26] although care must be taken to avoid processes such as multiple Andreev reflection and electron-electron scattering, which has been found to contribute to heat transport when superconducting Al leads are used to contact graphene [39].

Furthermore, for the same reasons listed above, which result in weak thermal coupling, the heat capacity of the electron gas is also expected to be minute. For

doped graphene, the heat capacity is expected to be $C_e = (2\pi^{3/2}k_B^2n^{1/2}T_e)/(3\hbar v_F)$ [7,18]. For perfectly pristine graphene, the heat capacity is expected to follow a $T^2 \ln T$ temperature dependence [19]; this is not the situation for a sample with disorder on a SiO₂ substrate. At 100 mK and with $n = 10^{11} \text{ cm}^{-2}$, one expects $C_e = 2.3 k_B$ for a $1 \times 1\text{-}\mu\text{m}$ flake. With this, combined with the thermal conductance, one can estimate the thermal time constant: $\tau = C_e/G_{\text{tot}}$. Assuming $G_{\text{tot}} \approx G_{\text{ep}}$, one expects the maximum thermal time constant to be $\tau = 10 \text{ ps}$ at 10 K, 1 ns at 1 K, and 10 μs at 10 mK. Because of the linear bands of graphene, and the correspondingly high Fermi temperature, the heat capacity of graphene can be 50 times lower than that of a heterostructure two-dimensional electron gas, for an assumed $n = 10^9 \text{ cm}^{-2}$.

III. NOISE THERMOMETRY AND SAMPLE FABRICATION

Given the expected very weak coupling and high-speed thermal response, we have implemented microwave-frequency noise thermometry to explore these delicate and wide-bandwidth thermal properties (Fig. 1). Noise thermometry has shown itself to be an excellent and nearly noninvasive probe of electron temperature for nanoscale devices with very minimal backaction heating [11,26,40]. Curiously, the dominant effect of this measurement scheme on the graphene sample is to provide a thermal conductance channel for cooling through the emission of photons into the measurement channel, G_{rad} . This radiative channel will be present for any electrical readout

scheme; however, in bolometers, which are sensed using electrical transport, heating due to Ohmic loss is the dominant perturbation for an optimized measurement [8,10].

The analysis of hot-electron bolometers with a resistive readout and operated with electrothermal feedback shows the optimized energy resolution to be $\Delta E \sim (2/\sqrt{\alpha})\Delta E_{\text{th}}$ [10,15,22,41], where $\alpha = (T/R)dR/dT$ and $\Delta E_{\text{th}} = \sqrt{4C_e k_B T}$ is the energy resolution limited by thermodynamic fluctuations of the bolometer. At 2 K, we measure $\alpha \approx 0.03$, which will limit the sensitivity of a resistively read-out graphene bolometer to a sensitivity $12\Delta E_{\text{th}}$. This situation becomes much worse at lower temperatures as both T and dR/dT decrease. Our analysis shows that an approach based upon noise thermometry is capable of approaching the thermodynamic limit, which leads us to believe that noise thermometry is preferable for experiments at very low temperatures.

Our graphene sample is fabricated using exfoliation onto a Si wafer coated with 285 nm of SiO₂; the single atomic layer thickness is confirmed using Raman spectroscopy [42]. The high-resistivity wafer (1–10 $\Omega\text{-cm}$ at 300 K) is insulating at the cryogenic temperature, and the electrical insulation minimizes the stray capacitance between the electrodes and the ground, which would otherwise capacitively load our impedance-matching network.

We match the relatively high impedance of a $15 \times 6.8 \mu\text{m}$ flake of graphene, 30 k Ω at the charge-neutrality point (CNP), to a 50 Ω measurement circuit using a lithographic, superconducting NbTiN LC network, which is placed a few millimeters from the graphene sample. The

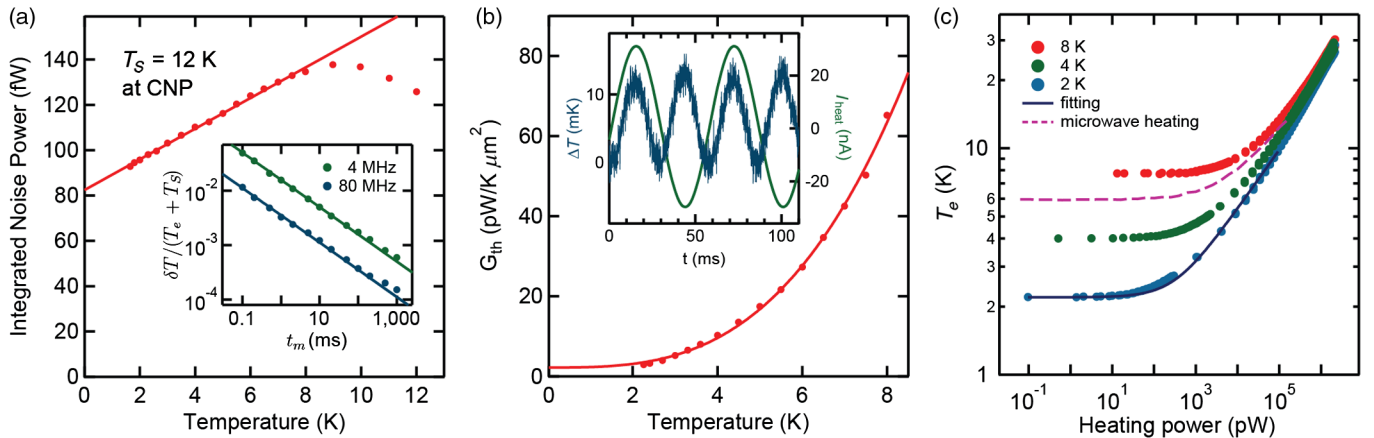


FIG. 2. (a) The integrated noise power versus refrigerator temperature, demonstrating the expected temperature dependence of the Johnson-noise signal. The deviation at temperatures above 8 K are due to the temperature dependence of the NbTiN inductor. The inset shows the precision of the noise thermometry taken with two measurement bandwidths, 4 and 80 MHz, versus integration time. A resolution of 100 ppm is achieved, in agreement with the Dicke radiometer formula (shown as lines). (b) The results of the differential thermal-conductance measurements. The inset shows a time trace, taken at 4 K, of the small heating current at 17.6 Hz, and the resulting 12-mK temperature oscillations at 35.2 Hz detected with the noise thermometer. The red curve is a power-law fit with exponent 2.7 ± 0.3 . (c) The results of applying large dc heating currents at various sample temperatures, T_p (points). The expected form is shown as the blue line. Also shown is the heating of the electron gas versus applied microwave power at 1.161 GHz, also showing a similar heating curve and demonstrating the microwave bolometric effect with graphene.

LC network ($L \approx 125$ nH, $C \approx 115$ aF) resonates at 1.161 GHz with a bandwidth of 80 MHz. As shown in the scattering parameter, S_{11} , in Fig. 1(d), absorption of microwave power is as high as 97% within the matched bandwidth.

In the same frequency band where we have engineered high absorption, the graphene is able to efficiently radiate Johnson noise; this is shown as the peak in the noise spectra at 1.2 GHz in Fig. 1(e). Analyzing these thermal noise spectrums below 8K in the matched bandwidth shows the expected linear dependence of the Johnson noise with temperature [Fig. 2(a)], i.e., $P_{\text{int}} = \mathcal{G}(k_B T + k_B T_S)$ where P_{int} is the integrated Johnson noise power, \mathcal{G} is the calibration gain for the noise thermometry, and T_S is the noise temperature of our system, due to the added noise of the amplifier. For $T > 8$ K, the LC matching network begins to substantially shift its frequency as the temperature approaches the superconducting transition temperature and kinetic inductance effects become significant [43]. The temperature-axis intercept of Fig. 2(a) determines $T_S \approx 12$ K.

The sensitivity of our noise thermometry, δT_e , follows the Dicke radiometer formula [44]: $\delta T_e / (T_e + T_S) = (B t_m)^{-1/2}$, where t_m is the measurement time, and B is the measurement bandwidth. For $B = 80$ MHz, this leads to an electron temperature noise power density of $\sqrt{\delta T_e} = 2 \text{ mK} / \sqrt{\text{Hz}}$ at 2 K. The inset of Fig. 2(a) shows the measured normalized standard deviation of the noise temperature versus the measurement time, plotted for two measurement bandwidths (4 and 80 MHz); the data follows the Dicke radiometer formula. We have recently realized much lower noise temperatures for our system of $T_S < 1$ K with the implementation of a wide bandwidth, nearly quantum-limited SQUID amplifier [45].

Ohmic contact is made using evaporated Au/Ti leads. However, an advantage of very high-frequency measurements is that high-transparency contacts are not required since capacitive coupling to a metal film deposited on the graphene can also be utilized. A 100-nm-thick, Au electrostatic gate is insulated from the graphene using a 100-nm-thick, overexposed electron beam resist (polymethyl methacrylate) as a dielectric [46] (see the blue area in the inset of Fig. 1(b)). Figure 1(c) shows the measured resistance of the graphene device versus the gate voltage, V_{gate} , with mobility of approximately $3500 \text{ cm}^2/\text{Vs}$ at a low temperature, corresponding to a mean-free path of about 20 nm. The charge-carrier density at the CNP is approximately $2 \times 10^{11} \text{ cm}^{-2}$, which is estimated by the width of the resistance maximum [12,47].

IV. MEASUREMENTS

We measure the thermal conductance of the electron gas by simultaneously applying currents through the graphene to produce Ohmic heating \dot{Q} while measuring the electronic noise temperature. We have investigated the heat

transfer in several limits: first, by measuring the differential thermal conductance with small quasistatic \dot{Q} at various temperatures; second, by using a larger dc-current bias which produces temperature changes comparable to or larger than the starting sample temperature; and finally, by using microwave-frequency heating currents. All of these measurements show similar results and are consistent with the existing theory of the electron-phonon coupling [5–7,31].

First, we impose a small oscillating current bias (I_{heat}) at 17.6 Hz, detect the resulting 35.2-Hz temperature oscillations of the electron gas in the limit where $\Delta T_e / T_e \approx 10^{-2}$, and then compute the differential thermal conductance: $G_{\text{th}} = \dot{Q} / \Delta T_e$ [Fig. 2(b)]. This data is well fitted with the expected form: $G_{\text{th}} = (p + 1) \Sigma A T^p$, with Σ and p as fitting parameters, and with values $0.07 \text{ W}/(\text{m}^2 \text{K}^3)$ and 2.7 ± 0.3 , respectively. The power-law exponent is near the theoretical expectation of $p = 3$. Figure 2(c) also shows the results of applying a wide range of dc current biases such that T_e can be much larger than T_p . We find this data to fit the expected form: $T_e = [\dot{Q} / (A \Sigma) + T_p^{p+1}]^{1/(p+1)}$ using Σ and p , which are found from the differential measurements.

We also apply a heating signal at 1.161 GHz, at the center frequency of our impedance-matching (LC) network where the absorption of the microwave power into the graphene is nearly complete [Fig. 1(d)], and measure the increase in the electron-gas temperature with the Johnson noise. This method also shows the same thermal conductance that we found with quasistatic heating and demonstrates graphene as a bolometer to microwave-frequency radiation. Using the measured sensitivity of the Johnson-noise thermometry and thermal conductance, the noise-equivalent power (NEP) of our graphene bolometer in this work is about $0.4 \text{ pW}/\sqrt{\text{Hz}}$ at 2 K. Below, we show that substantial improvements should be possible at lower temperatures and electron densities.

To probe the thermal time constant τ and reveal the heat capacity of the graphene, we utilize the microwave-frequency impedance-matching network together with the small temperature dependence of the electrical resistance of graphene [Fig. 1(c)]. This is a modified 3- ω method and is essentially a bolometric mixer [24].

We first apply a high-frequency oscillating current within the impedance-matching band to heat the sample; $\dot{Q} = I_{\text{heat}}^2(t) \cdot R(T_e) = I_{\text{heat}}^2 R(T_e) [1 + \cos(2\omega_{\text{heat}} t)] / 2$, where $\omega_{\text{heat}} = 2\pi \cdot 1.161 \text{ GHz}$. The DC component of the temperature change is observed through the Johnson noise of the sample, which is similar to the above thermal-conductance measurements. If the thermal time constant of the graphene electron gas satisfies $2\omega_{\text{heat}} \tau < 1$, then the temperature of the sample will oscillate at $2 \cdot \omega_{\text{heat}} = 2\pi \cdot 2.322 \text{ GHz}$. From our measurement of the G_{ep} and our expectation of the heat capacity, we expect $2\omega_{\text{heat}} \tau = 1$ for $T \approx 5.7 \text{ K}$. Given the weak dependence of the sample resistance on temperature, $dR/dT \sim 400 \text{ } \Omega/\text{K}$ at 2 K, the

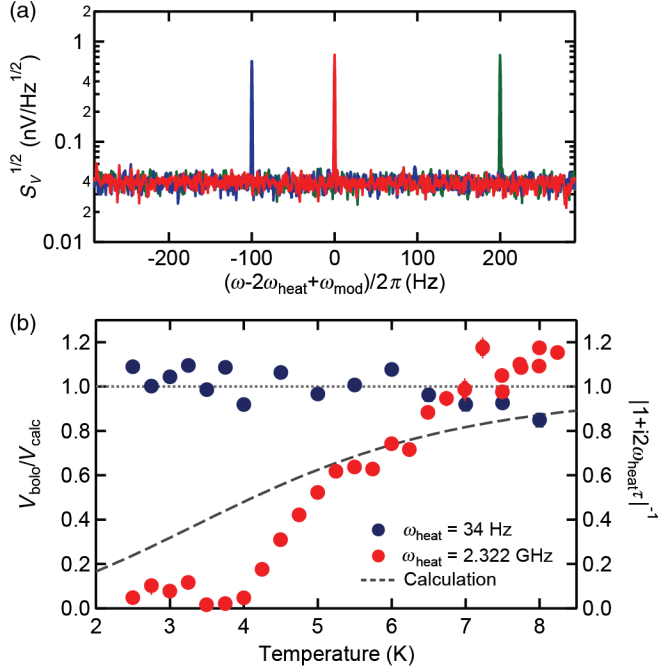


FIG. 3. Panel (a) shows the power spectral density, at the input of the HEMT, due to bolometric mixing. The central, 600-pV red tone is due to a heating signal at $\omega_{\text{heat}}/2\pi = 1.161$ GHz, which produces a temperature response at 2.322 GHz, which is then mixed down to $\omega_{\text{bolo}} = \omega_{\text{heat}} + 2\pi \cdot 1$ kHz using a small modulation tone at $\omega_{\text{mod}} = \omega_{\text{heat}} - 2\pi \cdot 1$ kHz. The blue spike, shifted down by 100 Hz, is the result of increasing the modulation tone by 100 Hz. The green spike, shifted up by 200 Hz, is due to increasing the heating tone by 100 Hz, validating the expected relationship: $\omega_{\text{bolo}} = 2\omega_{\text{heat}} - \omega_{\text{mod}}$. (b) A plot of the measured bolometric mixing tone normalized by our expected signal under the assumption that the graphene thermal time constant $\tau = 0$. The red points are measured with a heating tone of $\omega_{\text{heat}}/2\pi = 1.161$ GHz, the blue points are measured with $\omega_{\text{heat}}/2\pi = 17.6$ Hz, and both are measured with a modulation tone of 1.161 GHz–1 kHz. The dashed line shows the expected roll-off of the bolometric signal when $2\omega_{\text{heat}}/2\pi = 2.32$ GHz and $\tau = C_e/G_{\text{ep}}$.

impedance, $Z(\omega)$, will also oscillate at $2\omega_{\text{heat}}$ with T_e . By applying a second smaller modulation tone across the drain source of the graphene sample at $\omega_{\text{mod}} = \omega_{\text{heat}} - 1$ kHz, the impedance oscillations are then transduced into a very small voltage oscillation, typically 10–100 pV, and are mixed back into the range of our matching network; $\delta V(t) = (I_{\text{mod}} e^{-i\omega_{\text{mod}} t}) \cdot (\delta Z e^{-i2\omega_{\text{heat}} t})$, where a component of $\delta V(t)$ oscillates at $2\omega_{\text{heat}} - \omega_{\text{mod}}$. The power spectral density of the voltage across the graphene, S_V , in Fig. 3(a) shows that the mixing tone depends on the input frequencies as expected. See the Supplemental Material for more details of the mixing and signal processing [25].

For temperatures above 5 K, the observed amplitude and frequency of resulting mix tone agrees with our expectation due to a bolometric mixing effect. This demonstrates the detection of temperature oscillation of graphene sheet at 2.322 GHz. However, for temperatures below 5 K, we

observe a substantial decrease in the amplitude of the mixed tone, which is consistent with the expected roll-off due to the finite thermal-response time of the sheet due to the heat capacity [Fig. 3(b)]. Figure 3(b) shows the measured bolometric mixing tone in graphene, V_{bolo} , normalized to the theoretical mixing tone value, V_{calc} , if $\tau = 0$. (See the Supplemental Material for mathematical details [31].) As a control of the experiment, we have performed the same measurement procedures with ω_{heat} set to $2\pi \times 17.6$ Hz, and $\omega_{\text{mod}} = 2\pi \cdot 1.160999$ GHz. No roll-off of the bolometric mixed tone at $\omega_{\text{mod}} + 2 \cdot 2\pi \cdot 17.6$ Hz versus temperature was observed, which is as expected since $2\omega_{\text{heat}}\tau_{\text{th}} \ll 1$ in this case. At 5.25 K, we calculate a heat capacity of $12000k_B$, which is comparable to the smallest heat capacity measured to date [9]. We also believe this to be the first measurement of the heat capacity of a two-dimensional electron gas at zero field.

V. DISCUSSION

We compare our thermal-conductance data to the existing theoretical predications of the electron-phonon coupling [5–7]. Using 30 eV as the deformation potential from the electrical-transport measurements in single-layer graphene [12,13,30], we find that our data is consistent with an effective charge carrier density of $4.9 \times 10^{11} \text{ cm}^{-2}$. This is within a factor of 2.5 of the charge density estimated from the measurements of the resistance as a function of the gate voltage ($2 \times 10^{11} \text{ cm}^{-2}$). The agreement of our data to the theory, both in magnitude and in temperature dependence, is somewhat surprising for two reasons. First, we make our measurements at the CNP where the electron density is a result of a large disorder potential that is typical with SiO_2 substrates [23]. Second, our sample is deep in the diffusive limit, i.e., $k_F l_e \ll 1$. It is known from work on conventional two-dimensional electron-gas structures that this diffusive limit and screening can substantially alter the electron-phonon coupling [48]. To date, we are aware of no published literature on the electron-phonon coupling in graphene in the diffusive limit and near the CNP. Theoretical work on this limit will be very useful.

The Wiedemann-Franz thermal conductance estimated here is based on that of a two-dimensional electron gas [16]. At a low charge-carrier density, theories have suggested that deviations from the WF relationship are due to the relativistic band structure [17]. This physics can be probed by performing this experiment at a lower temperature.

The data we have gathered on the thermal-transport and thermodynamic properties of graphene from 2–30 K and the sensitivity of our wide-bandwidth thermometry system motivates an estimation of the sensitivity of graphene as a bolometer and photon detector at lower temperatures [8,10]. Figure 4 shows the expected sensitivity as a bolometer versus noise bandwidth for various temperatures, where the NEP is given by $\text{NEP} = G_{\text{tot}} \cdot \sqrt{S_T}$, where S_T is the noise spectral density of the noise thermometer. Given

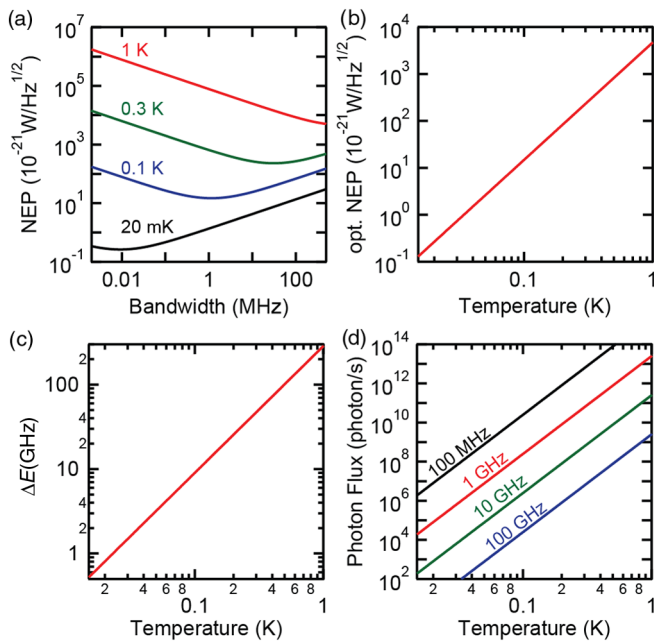


FIG. 4. (a) The expected sensitivity of graphene as a bolometer assuming $n = 10^9 \text{ cm}^{-2}$ and $A = 10^{-11} \text{ m}^2$ versus the coupling bandwidth, for various cryogenic operating temperatures, with (b) the optimal value of NEP versus temperature. (c) The expected energy sensitivity to single photons. (d) The threshold for detection of shot noise of an incident microwave field of various frequencies.

the minute heat capacity for $T < 1 \text{ K}$, the temperature resolution is expected to be limited by the thermodynamic fluctuations of the energy of the electron gas [8,49]; $\langle \Delta T_e^2 \rangle = k_B T_e^2 / C$, which gives $S_T(\omega) = 4\tau k_B T_e^2 / \{C[1 + (\tau\omega)^2]\}$. The maximum sensitivity versus measurement bandwidth is a result of the balance between gaining resolution in the noise thermometry by increasing the measurement band, and increasing the thermal response by decreasing G_{rad} . As is clear from Figs. 4(a) and 4(b), a graphene-based bolometer may exceed the sensitivity of the current state-of-the-art bolometers developed for far-infrared or submillimeter-wave astronomy with a sensitivity of $6 \times 10^{-20} \text{ W}/\sqrt{\text{Hz}}$ and a thermal time constant of $\tau = 300 \text{ ms}$ [20], an improvement in bandwidth of approximately 5 orders of magnitude.

As a photon detector and calorimeter, the expected energy resolution is given by [10,11] $\Delta E = \text{NEP} \cdot \sqrt{\tau}$. Given the exceptionally fast thermal time constant, one expects single-photon sensitivity to gigahertz photons [Fig. 4(c)]. For astrophysical applications in terahertz spectroscopy, one expects an energy resolution of four parts in 100 at 300 mK for an absorbed 1 THz photon. This satisfies the instrument resolution requirements for future NASA missions (BLISS) at ^3He -refrigerator temperatures [50]. Compared to the recently proposed superconducting hot-electron photon counter for THz applications at 300 mK [21], the NEP of graphene-based bolometers is about 10

times less sensitive. However, the energy resolution for graphene is expected to be about 7 times better. In this way, graphene bolometers are a possible solution for low-flux photon counting in the THz regime [21]. At 10 mK, the intriguing possibility to observe single 800 MHz photons appears possible.

Furthermore, for high photon flux, \dot{n} , the quantization of the field produces shot noise on the incoming power: $S_{\text{shot}} = 2(\hbar\omega)^2 \dot{n} \text{ W}^2/\text{Hz}$. For sufficiently high microwave photon flux, this noise will dominate the temperature fluctuations of the sample [Fig. 4(d)]. At 100 mK, and with 10-GHz photons, for fluxes greater than 10^6 photons/s, the noise of the bolometer should be dominated by the shot noise of the microwave field. In this way, graphene would act as a photodetector for microwaves, having a square-law response and being absorptive and sensitive to the shot noise of the incoming field. We know of no other microwave detector that has these characteristics and this would open the door to novel quantum optics experiments with microwave photons [51].

ACKNOWLEDGMENTS

We acknowledge help with the microfabricated LC resonators from M. Shaw, and helpful conversations with P. Kim, J. Hone, D. Prober, E. Henriksen, J. P. Eisenstein, A. Clerk, P. Hung, E. Wollman, A. Weinstein, B.-I. Wu, D. Nandi, J. Zmuidzinas, J. Stern, W.H. Holmes, and P. Echternach. This work has been supported by the FCRP Center on Functional Engineering Nano Architectonics (FENA) and U.S. NSF Contract No. (DMR-0804567). We are grateful to G. Rossman for the use of a Raman spectroscopy setup. Device fabrication was performed at the Kavli Nanoscience Institute (Caltech) and at the Micro Device Laboratory (NASA/JPL).

Note added.—During the writing of this work, we became aware of three other experimental works that touch on some of these concepts [52].

- [1] A.H. Castro Neto, F. Guinea, N.M.R. Peres, K.S. Novoselov, and A.K. Geim, *The Electronic Properties of Graphene*, *Rev. Mod. Phys.* **81**, 109 (2009); S. Das Sarma, S. Adam, E.H. Hwang, and E. Rossi, *Electronic Transport in Two-Dimensional Graphene*, *Rev. Mod. Phys.* **83**, 407 (2011).
- [2] A.A. Balandin, *Thermal Properties of Graphene and Nanostructured Carbon Materials*, *Nature Mater.* **10**, 569 (2011).
- [3] A.A. Balandin, S. Ghosh, W. Bao, I. Calizo, D. Teweldebrhan, F. Miao, and C.N. Lau, *Superior Thermal Conductivity of Single-Layer Graphene*, *Nano Lett.* **8**, 902 (2008); J.H. Seol, I. Jo, A.L. Moore, L. Lindsay, Z.H. Aitken, M.T. Pettes, X. Li, Z. Yao, R. Huang, D. Broido, N. Mingo, R.S. Ruoff, and L. Shi, *Two-Dimensional Phonon Transport in Supported Graphene*, *Science* **328**, 213 (2010); D.L. Nika, E.P.

- Pokatilov, A.S. Askerov, and A.A. Balandin, *Phonon Thermal Conduction in Graphene: Role of Umklapp and Edge Roughness Scattering*, *Phys. Rev. B* **79**, 155413 (2009).
- [4] Y.M. Zuev, W. Chang, and P. Kim, *Thermoelectric and Magnetothermoelectric Transport Measurements of Graphene*, *Phys. Rev. Lett.* **102**, 096807 (2009); P. Wei, W. Bao, Y. Pu, C.N. Lau, and J. Shi, *Anomalous Thermoelectric Transport of Dirac Particles in Graphene*, *ibid.* **102**, 166808 (2009).
- [5] W.-K. Tse and S. Das Sarma, *Energy Relaxation of Hot Dirac Fermions in Graphene*, *Phys. Rev. B* **79**, 235406 (2009).
- [6] S.S. Kubakaddi, *Interaction of Massless Dirac Electrons with Acoustic Phonons in Graphene at Low Temperatures*, *Phys. Rev. B* **79**, 075417 (2009).
- [7] J.K. Viljas and T.T. Heikkilä, *Electron-Phonon Heat Transfer in Monolayer and Bilayer Graphene*, *Phys. Rev. B* **81**, 245404 (2010).
- [8] J.C. Mather, *Bolometer Noise: Nonequilibrium Theory*, *Appl. Opt.* **21**, 1125 (1982).
- [9] J. Wei, D. Olaya, B.S. Karasik, S.V. Pereverzev, A.V. Sergeev, and M.E. Gershenson, *Ultrasensitive Hot-Electron Nanobolometers for Terahertz Astrophysics*, *Nature Nanotech.* **3**, 496 (2008).
- [10] S.H. Moseley, J.C. Mather, and D. McCammon, *Thermal Detectors as X-Ray Spectrometers*, *J. Appl. Phys.* **56**, 1257 (1984).
- [11] M.L. Roukes, *Yoctocalorimetry: Phonon Counting in Nanostructures*, *Physica (Amsterdam)* **263–264B**, 1 (1999).
- [12] K.I. Bolotin, K.J. Sikes, J. Hone, H.L. Stormer, and P. Kim, *Temperature-Dependent Transport in Suspended Graphene*, *Phys. Rev. Lett.* **101**, 096802 (2008).
- [13] J.-H. Chen, C. Jang, S. Xiao, M. Ishigami, and M.S. Fuhrer, *Intrinsic and Extrinsic Performance Limits of Graphene Devices on SiO₂*, *Nature Nanotech.* **3**, 206 (2008).
- [14] J.C. Mather, *Bolometers: Ultimate Sensitivity, Optimization, and Amplifier Coupling*, *Appl. Opt.* **23**, 584 (1984).
- [15] D. McCammon, in *Cryogenic Particle Detection*, edited by C. Enss (Springer, New York, 2005), p. 1–34.
- [16] V.P. Gusynin and S.G. Sharapov, *Magnetic Oscillations in Planar Systems with the Dirac-Like Spectrum of Quasiparticle Excitations. II. Transport Properties*, *Phys. Rev. B* **71**, 125124 (2005); B. Dóra and P. Thalmeier, *Magnetotransport and Thermoelectricity in Landau-Quantized Disordered Graphene*, *ibid.* **76**, 035402 (2007); M. Trushin and J. Schliemann, *Minimum Electrical and Thermal Conductivity of Graphene: A Quasiclassical Approach*, *Phys. Rev. Lett.* **99**, 216602 (2007); W. Long, H. Zhang, and Q.-F. Sun, *Quantum Thermal Hall Effect in Graphene*, *Phys. Rev. B* **84**, 075416 (2011).
- [17] K. Saito, J. Nakamura, and A. Natori, *Ballistic Thermal Conductance of a Graphene Sheet*, *Phys. Rev. B* **76**, 115409 (2007); T. Löfwander and M. Fogelström, *Impurity Scattering and Mott's Formula in Graphene*, *ibid.* **76**, 193401 (2007); T. Stauber, N. Peres, and F. Guinea, *Electronic Transport in Graphene: A Semiclassical Approach Including Midgap States*, *ibid.* **76**, 205423 (2007); M. Müller, L. Fritz, and S. Sachdev, *Quantum-Critical Relativistic Magnetotransport in Graphene*, *ibid.* **78**, 115406 (2008); M. Foster and I. Aleiner, *Slow Imbalance Relaxation and Thermoelectric Transport in Graphene*, *ibid.* **79**, 085415 (2009).
- [18] M.R. Ramezani, M.M. Vazifeh, R. Asgari, M. Polini, and A.H. MacDonald, *Finite-Temperature Screening and the Specific Heat of Doped Graphene Sheets*, *J. Phys. A* **42**, 214015 (2009).
- [19] O. Vafek, *Anomalous Thermodynamics of Coulomb-Interacting Massless Dirac Fermions in Two Spatial Dimensions*, *Phys. Rev. Lett.* **98**, 216401 (2007).
- [20] M. Kenyon, P.K. Day, C.M. Bradford, J.J. Bock, and H.G. Leduc, *Electrical Properties of Background-Limited Membrane-Isolation Transition-Edge Sensing Bolometers for Far-IR/Submillimeter Direct-Detection Spectroscopy*, *J. Low Temp. Phys.* **151**, 112 (2008).
- [21] B.S. Karasik and A.V. Sergeev, *THz Hot-Electron Photon Counter*, *IEEE Trans. Appl. Supercond.* **15**, 618 (2005).
- [22] B.S. Karasik, A.V. Sergeev, and D.E. Prober, *Nanobolometers for THz Photon Detection*, *IEEE Trans. Terahertz Sci. Tech.* **1**, 97 (2011).
- [23] J. Martin, N. Akerman, G. Ulbricht, T. Lohmann, J.H. Smet, K. von Klitzing, and A. Yacoby, *Observation of Electron-Hole Puddles in Graphene Using a Scanning Single-Electron Transistor*, *Nature Phys.* **4**, 144 (2008); Y. Zhang, V.W. Brar, C. Girit, A. Zettl, and M.F. Crommie, *Origin of Spatial Charge Inhomogeneity in Graphene*, *ibid.* **5**, 722 (2009).
- [24] D.E. Prober, *Superconducting Terahertz Mixer Using a Transition-Edge Microbolometer*, *Appl. Phys. Lett.* **62**, 2119 (1993).
- [25] See Supplemental Material at <http://link.aps.org/supplemental/10.1103/PhysRevX.2.031006> for details in fabrication, experimental setup, microwave circuit modeling, graphene thermal model, data processing, and calculations.
- [26] K.C. Schwab, E.A. Henriksen, J.M. Worlock, and M.L. Roukes, *Measurement of the Quantum of Thermal Conductance*, *Nature (London)* **404**, 974 (2000).
- [27] J.B. Pendry, *Quantum Limits to the Flow of Information and Entropy*, *J. Phys. A* **16**, 2161 (1983); M. Meschke, W. Guichard, and J.P. Pekola, *Single-Mode Heat Conduction by Photons*, *Nature (London)* **444**, 187 (2006); D.R. Schmidt, R.J. Schoelkopf, and A.N. Cleland, *Photon-Mediated Thermal Relaxation of Electrons in Nanostructures*, *Phys. Rev. Lett.* **93**, 045901 (2004).
- [28] M.L. Roukes, M.R. Freeman, R.S. Germain, R.C. Richardson, and M.B. Ketchen, *Hot-Electrons and Energy-Transport in Metals at Millikelvin Temperatures*, *Phys. Rev. Lett.* **55**, 422 (1985).
- [29] E.H. Hwang and S. Das Sarma, *Acoustic Phonon Scattering Limited Carrier Mobility in Two-Dimensional Extrinsic Graphene*, *Phys. Rev. B* **77**, 115449 (2008).
- [30] D.K. Efetov and P. Kim, *Controlling Electron-Phonon Interactions in Graphene at Ultrahigh Carrier Densities*, *Phys. Rev. Lett.* **105**, 256805 (2010).
- [31] R. Bistritzer and A.H. MacDonald, *Electronic Cooling in Graphene*, *Phys. Rev. Lett.* **102**, 206410 (2009).

- [32] B. Huard, N. Stander, J. A. Sulpizio, and D. Goldhaber-Gordon, *Evidence of the Role of Contacts on the Observed Electron-Hole Asymmetry in Graphene*, *Phys. Rev. B* **78**, 121402 (2008).
- [33] K. Nagashio, T. Nishimura, K. Kita, and A. Toriumi, *Contact Resistivity and Current Flow Path at Metal/Graphene Contact*, *Appl. Phys. Lett.* **97**, 143514 (2010).
- [34] J. Horng, C.-F. Chen, B. Geng, C. Girit, Y. Zhang, Z. Hao, H. Bechtel, M. Martin, A. Zettl, M. Crommie, Y. Shen, and F. Wang, *Drude Conductivity of Dirac Fermions in Graphene*, *Phys. Rev. B* **83**, 165113 (2011).
- [35] Z. Chen, W. Jang, W. Bao, C.N. Lau, and C. Dames, *Thermal Contact Resistance between Graphene and Silicon Dioxide*, *Appl. Phys. Lett.* **95**, 161910 (2009).
- [36] S.S. Mohan, M.D. Hershenson, S.P. Boyd, and T.H. Lee, *Simple Accurate Expressions for Planar Spiral Inductances*, *IEEE J.: Solid-State Circuits* **34**, 1419 (1999).
- [37] R. Danneau, F. Wu, M. F. Craciun, S. Russo, M. Y. Tomi, J. Salmilehto, A. F. Morpurgo, and P. J. Hakonen, *Shot Noise in Ballistic Graphene*, *Phys. Rev. Lett.* **100**, 196802 (2008); L. DiCarlo, J.R. Williams, Y. Zhang, D.T. McClure, and C.M. Marcus, *Shot Noise in Graphene*, *ibid.* **100**, 156801 (2008).
- [38] A. H. Steinbach, J.M. Martinis, and M.H. Devoret, *Observation of Hot-Electron Shot Noise in a Metallic Resistor*, *Phys. Rev. Lett.* **76**, 3806 (1996).
- [39] J. Voutilainen, A. Fay, P. Hakkinen, J.K. Viljas, T.T. Heikkila, and P.J. Hakonen, *Energy Relaxation in Graphene and its Measurement with Supercurrent*, *Phys. Rev. B* **84**, 045419 (2011).
- [40] L. Spietz, K. W. Lehnert, I. Siddiqi, and R. J. Schoelkopf, *Primary Electronic Thermometry Using the Shot Noise of a Tunnel Junction*, *Science* **300**, 1929 (2003).
- [41] K.D. Irwin, *An Application of Electrothermal Feedback for High-Resolution Cryogenic Particle-Detection*, *Appl. Phys. Lett.* **66**, 1998 (1995).
- [42] A.C. Ferrari, J.C. Meyer, V. Scardaci, C. Casiraghi, M. Lazzeri, F. Mauri, S. Piscanec, D. Jiang, K. S. Novoselov, S. Roth, and A. K. Geim, *Raman Spectrum of Graphene and Graphene Layers*, *Phys. Rev. Lett.* **97**, 187401 (2006).
- [43] R. Meservey and P.M. Tedrow, *Measurements of Kinetic Inductance of Superconducting Linear Structures*, *J. Appl. Phys.* **40**, 2028 (1969); A. J. Annunziata, D. F. Santavica, L. Frunzio, G. Catelani, M. J. Rooks, A. Frydman, and D.E. Prober, *Tunable Superconducting Nanoinductors*, *Nanotechnology* **21**, 445202 (2010).
- [44] R.H. Dicke, *The Measurement of Thermal Radiation at Microwave Frequencies*, *Rev. Sci. Instrum.* **17**, 268 (1946).
- [45] M. Muck, J.B. Kycia, and J. Clarke, *Superconducting Quantum Interference Device as a Near-Quantum-Limited Amplifier at 0.5 GHz*, *Appl. Phys. Lett.* **78**, 967 (2001).
- [46] H. Duan, J. Zhao, Y. Zhang, E. Xie, and L. Han, *Preparing Patterned Carbonaceous Nanostructures Directly by Overexposure of PMMA Using Electron-Beam Lithography*, *Nanotechnology* **20**, 135306 (2009); E. A. Henriksen and J.P. Eisenstein, *Measurement of the Electronic Compressibility of Bilayer Graphene*, *Phys. Rev. B* **82**, 041412 (2010).
- [47] C.R. Dean, A.F. Young, I. Meric, C. Lee, L. Wang, S. Sorgenfrei, K. Watanabe, T. Taniguchi, P. Kim, K.L. Shepard, and J. Hone, *Boron Nitride Substrates for High-Quality Graphene Electronics*, *Nature Nanotech.* **5**, 722 (2010).
- [48] A. V. Sergeev and V. Mitin, *Electron-Phonon Interaction in Disordered Conductors: Static and Vibrating Scattering Potentials*, *Phys. Rev. B* **61**, 6041 (2000).
- [49] T. C. P. Chui, D. R. Swanson, M. J. Adriaans, J. A. Nissen, and J. A. Lipa, *Temperature-Fluctuations in the Canonical Ensemble*, *Phys. Rev. Lett.* **69**, 3005 (1992).
- [50] D.J. Benford, M.J. Amato, J.C. Mather, S.H. Moseley, and D.T. Leisawitz, *Mission Concept for the Single Aperture Far-Infrared (SAFIR) Observatory*, *Astrophys. Space Sci.* **294**, 177 (2004).
- [51] T. Rocheleau, T. Ndukum, C. Macklin, J.B. Hertzberg, A. A. Clerk, and K. C. Schwab, *Preparation and Detection of a Mechanical Resonator Near the Ground State of Motion*, *Nature (London)* **463**, 72 (2010).
- [52] J. Yan, M. H. Kim, J. A. Elle, A. B. Sushkov, G. S. Jenkins, H. M. Milchberg, M. S. Fuhrer, and H. D. Drew, *Dual-Gated Bilayer Graphene Hot Electron Bolometer*, *Nature Nanotech.* **7**, 472 (2012); H. Vora, P. Kumaravadivel, B. Nielsen, and X. Du, *Bolometric Response in Graphene Based Superconducting Tunnel Junctions*, *Appl. Phys. Lett.* **100**, 153507 (2012); A.C. Betz, F. Violla, D. Brunel, C. Voisin, M. Picher, A. Cavanna, A. Madouri, G. Fève, J.M. Berroir, B. Plaçaïs, and E. Pallecchi, *Hot Electron Cooling by Acoustic Phonons in Graphene*, [arXiv:1203.2753v1](https://arxiv.org/abs/1203.2753v1).